International Journal of Science and Engineering Applications
Volume 10-Issue 11, 152 - 162, 2021, ISSN:- 2319 - 7560

Finite Element Analysis of End Effector for an Automated Equipment of High-Speed Forming of Thin-Layered Composite Materials

Jake Reeves
Department of Mechanical Engineering
Mississippi State University
Mississippi State, MS 39762,
United States

Dam Kim
Department of Mechanical Engineering
Mississippi State University
Mississippi State, MS 39762,
United States

Yucheng Liu
Department of Mechanical Engineering
South Dakota State University
Brookings, SD, 57007, United States

Youssef Hammi
Department of Mechanical Engineering
Mississippi State University
Mississippi State, MS 39762
United States

Abstract: The present study examines the design of an automated equipment system that will be able to form thin-layered composite materials over a highly complex shape in a very short time interval. The end effector is one of the most essential components of the automated equipment. It is connected to an assembly which is connected to a motorized arm which controls its motion in the y- and z-directions. The end effector is a component that holds an air pressurized fire hose, which is being used as the forming device of this automated forming device. As a result, the end effector will have to be able to hold and contain a highly pressurized fire hose while applying forces in a variety of directions depending on the shape of the forming mandrel. A computational approach using finite element analysis (FEA) was used to examine the end effector materials and the assembly to confirm that they are robust enough to withstand the internal and external stresses and forces without failure or permanent deformation of the end effector materials, forces which are created from the pressurized fire hose and reactive force on the fire hose from the pressure being applied to an independent tool. This means that the automated equipment is capable of forming complex composite laminates in a rapid time without resulting defects.

Keywords: Finite element analysis (FEA), automated equipment, end effector, ethylene propylene diene monomer (EPDM) rubber, composite material

1. INTRODUCTION

The purpose of this study is to determine the stresses and deformation that the end effector of an automated equipment system for high-speed forming thin-layered composite materials will incur during the operation of the system. This automated equipment system will be employed to form the thin-layered composite materials with a highly complex shape in fast cycle times. The system is made up of several components and this study will focus on the end effector, a key component which consists of actuated arm end plates, a rod end attach block, a base plate, a pivot rod end assembly, shaft blocks, a hose plate assembly, and a fire hose (Fig. 1).

In composites manufacturing there are several different types of material equipment; two being material laying equipment and material forming equipment. Material laying equipment are CNC machines with programmable axis movements, rack and pinion and/or linear motor axis drives, and "delivery heads" to dispense the prepreg composite materials. Prepreg material is a carbon fiber material pre-impregnated with resin. The machines are programmed to follow the exact contour of the part tool and lay the prepreg materials onto the tool surface. Automated Tape Layers (ATL) and Automated Fiber Placement (AFP) are commonly material laying equipment used for many aerospace applications like wing skins, spars, ribs, stringers, and fixed trailing edges. ATL and AFP systems are primarily the "material delivery head" technology as there is nothing magic about machine tools. CNC machine tool technology has been used for many years [1].

This research closely aligns with material forming equipment which takes the material that has been laid into flat shapes and pushes it into complex shapes and geometries. Forming equipment often work hand in hand with materials laying equipment, being one of the very next steps in the process. The process of forming composite material in this research process is an automated machine forming machine that takes a flat single ply or thin laminate of prepreg material and presses it into contour and shape. Then repeating the process over and over again on top of itself until the full thickness of the desired laminate is reached. The basis of the end effector is from the historical forming processes developed by The Boeing Company [2-3]. The reason that these methods have been targeted for this research is due its proven effectiveness to form composite materials. Composite materials are extremely difficulty while maintaining laminate quality.

Forming prepreg composite laminates are most subjected to fiber wrinkles during the forming process if they are not properly supported and constrained. Fiber wrinkles in carbon fiber reinforced polymer (CFRP) materials have shown reduction in tensile strengths by 36-40% [4]. With such drastic decreases in strength, it is extremely important to pay close attention to the part quality when manufacturing CFRP parts.

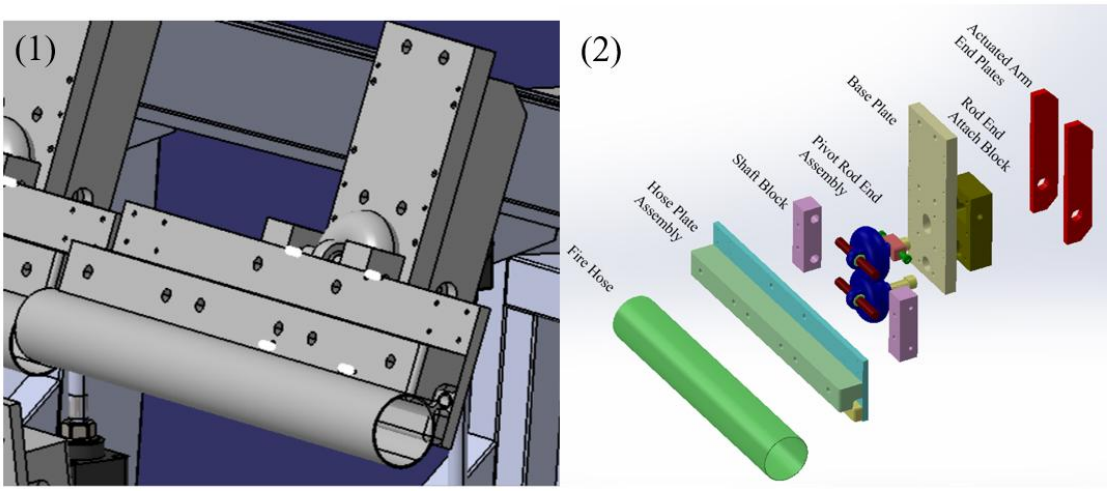

Figure 1. (L) an end effector assembly; (R) its component list

The radius of curvature that the fire hose of the end effector will have to go over will range from 1000 in and 6000 in (25.4 m to 152.4 m). This is the current engineering design that covers most of the curvatures for commercial airplane wing stringers. For this study we will focus on one segment of the end effector which is 23.5 in (59.69 cm) long. The reason of focusing on one section is that the results should be the same but the computing time can be reduced by only looking at one section instead of the entire assembly.

The design of the end effector system is critical in order to ensure that the fire hose, hose plate and assembly components will be able to withstand the different stresses and deformation that will be subject to while fabricating high quality composite laminates. The stresses will be the internal pressure applied to the fire hose and any deflection that the hose plate assembly might incur from the internal fire hose pressure combined with the z-directional applied forced reacted against the fire hose from forming against the forming contour tool.

This equipment will only be handling uncured composite materials; uncured composites are the composite materials that have not yet gone through an autoclave process with heat and pressure to put the laminate in its final cured state. The laminate will have come from an ATL machine, laminating a single ply or thin laminate on a carrier film to be discarded or recycled after each forming cycle. In a production environment, the forming cycles are repeated until maximum thickness is reached and then the formed laminates are assembled together and placed on a cure tool with caul plates and cured into shape. There are several key factors in shaping uncured composite materials; including composite material type (matrix and resin material properties), thickness of composite plies, tooling/support of the composite materials, overall forming pressure and speed as well as consistent/uniform pressure and speed. If the laminates are formed while not adjusting the parameters to these key factors, wrinkles will be induced into the fabricated composite materials which drastically affect the strength and performance of the final composite parts. Some wrinkles are allowed under special circumstances, but typical research and testing is performed with the goal to completely eliminate and prevent any wrinkles from forming. In this research the goal is to form laminates into contour with no wrinkles present.

Figure 2. Wrinkles appear on uncured composite laminates

Other common defects in inadequately formed composites include non-uniform laminate thickness (too thick or too thin), porosity, delamination, and marcelling, etc. To prevent those defects from occurring the equipment needs to be properly calibrated to apply an appropriate amount of pressure on the composite material so that the fire hose can hold the composite laminate in place while forming it over the contour of the forming tool and over a ¼" (6.35 mm) radius which is built into the tool. This radius is part of the wing stringer configuration. The fire hose will be inflated to about 10-15 PSI (~69-103 kPa) and will apply a downward force of 1000-2000 pounds (~4500-9000 N) onto laminate which is on a contoured forming tool. The steps for this automated forming process are illustrated in Fig. 3.

Step 1: Place a laminate on the contoured forming blocks.

Step 2: The pressurized fire hose is lowered onto the laminate and clamps the laminate into a place on the contoured forming blocks with a downward force of 4500-9000 N.

Step 3: The pressurized forming blocks sweep out in the horizontal direction while maintaining a constant pressure on the contoured forming blocks.

Step 4: The pressurized fire hose sweeps around the radius of the contoured forming blocks.

Step 5: The pressurized fire hose sweeps down the vertical face of the contoured forming blocks. This is the final forming step and will be repeated until the full thickness of the laminate is achieved.

Step 6: The forming blocks are rotated for assembling the two formed laminates and preparing for cure. This step is performed after all plies of the laminate have been formed over the contoured forming blocks.

Step 7: The forming blocks are in the assembly position.

Step 8: The forming blocks are mechanically clamped together and transferred to the cure tool to be staged for the autoclave.

Among the below steps, the laminate is formed to the shape and contour of the forming blocks with the downward force from the fire hose through steps 2 to 5. The steps 6 to 8 are post forming steps and can be performed offline so they do not interrupt future forming processes on this automated forming equipment.

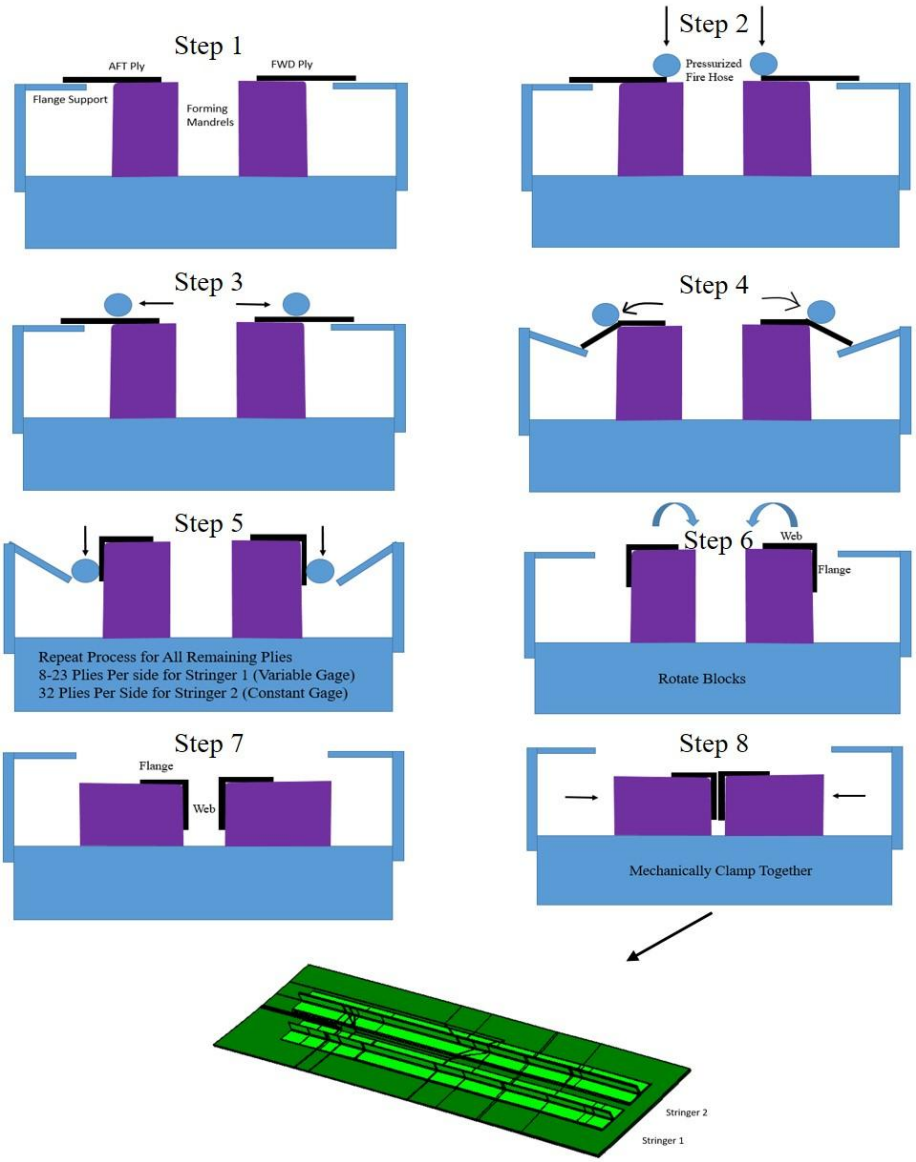

Figure 3. Forming process

2. PROBLEM DESCRIPTION

As mentioned before, this study focuses on the design of the end effector, which is a group of components that are responsible for touching/forming the composite laminate (Fig. 4) [5].

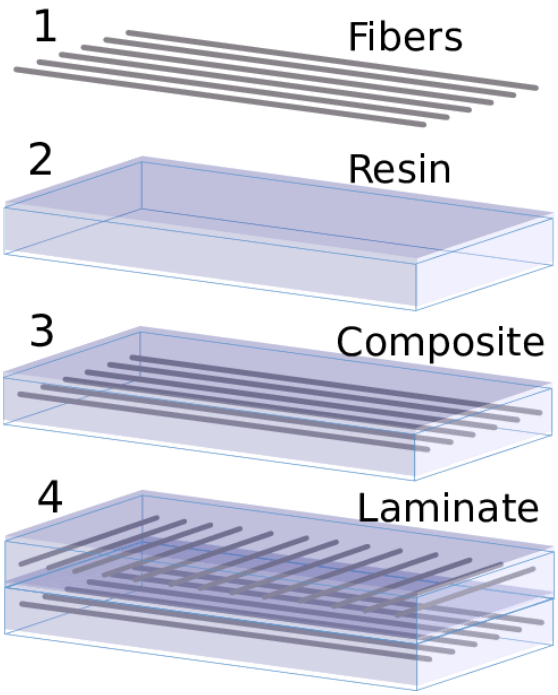

Figure 4. Schematic Picture of a Composite Laminate [5]

The end effector is made up of several 6061 aluminum pieces (actuated arm end plates, a rod end attach block, a base plate, a pivot rod end assembly, shaft blocks, and a hose plate assembly) and an inflatable fire hose. The inflatable fire hose is made from ethylene propylene diene monomer (EPDM) rubber that has an external fabric weave for strength and durability. A fire hose was chosen to act as the composite forming agent due to its high durability yet compliant structure.

Figure 5. A fire hose with a 4" (101.6) diameter

This study will be examining the non-linear analyses of the end effector inflated fire hose as well as the analyses of the aluminum plate and fittings that are part of the end effector assembly. The goals of the analysis will be computational analysis that will precede experimental trials.

3. AUTOMATED FORMING EQUIPMENT

A computer-aided design (CAD) model for the automated system was created using CATIA, as shown in Fig. 6. That figure also illustrates how this system can form two laminates simultaneously.

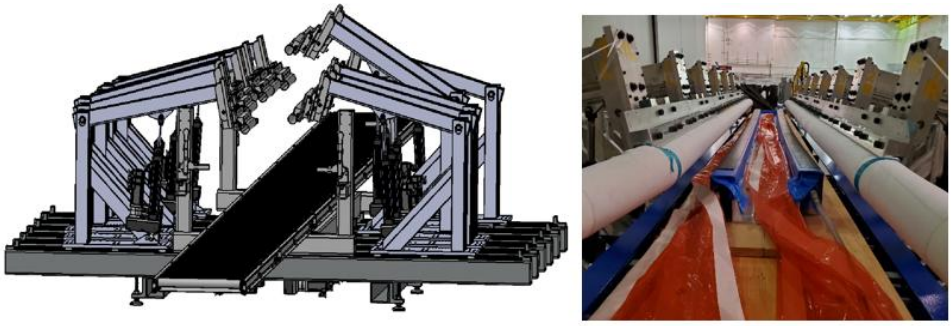

Figure 6. (L) A CAD model of the forming machine; (R) actual prototype of the forming machine

It can be seen from Fig. 6 that each end effector can move independently to one another but it is important to note that there will be a fire hose bridging the gap in between each of the end effector. The independent motions of individual end effectors make it possible to program the motions of the end effectors to move and independent of one another and form a laminate over different contours, joggles and asymmetric features.

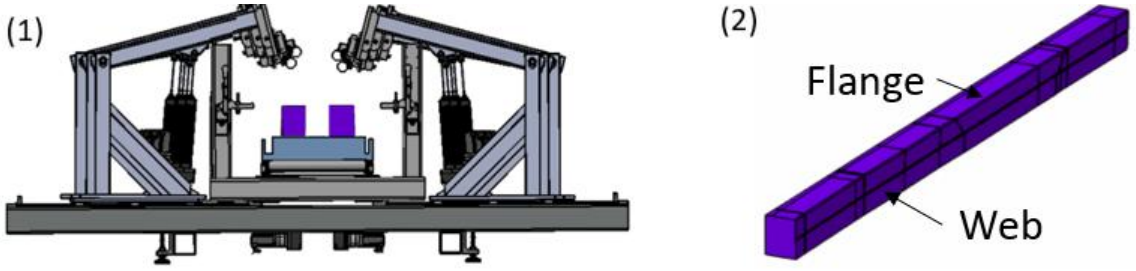

Figure 7. (L) The forming machine with forming mandrels; (R) and a contoured forming mandrel

The forming mandrels are approximately 135" (3.43 m) long and have a radius of curvature between 1000 in and 6000 in (25.4 m to 152.4 m) depending on the specific part that is being fabricated. The contoured forming mandrel is a tool that supports the laminate and has the features and contours of a specific commercial airplane wing stringer. This is the tooled surface the shapes the wing stringer. It has two surfaces that will contact the composite laminate. The top surface is the flange and the vertical surface is the web, and there is a 0.25 in (0.635 cm) radius that connects the two surfaces. There also are several joggles and steps on the surfaces of the mandrel. These features are the primary reasons that make it very difficult to create an automated forming equipment to form this specific composite structure because it is almost impossible to have such a machine roll over these surfaces without inducing any wrinkles on the laminate.

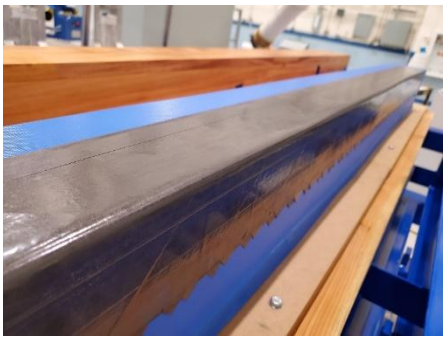

Figure 8. A composite laminate over a forming Mandrel

The machine will be forming at a very high speed as well. The primary reason that it needs to operate at a high speed is to prove the opportunity for this equipment in production by demonstrating faster cycle times to produce a wing stringer over alternative fabrication methods. The target speed is approximately 24 in/min (61 cm/min). For parts with highly complex geometries, this is an extremely fast speed but with increased speed usually comes the increased the chance of manufacturing poor quality laminates. Determining the proper end effector materials and assembly method will help ensure a high quality laminate at high speeds.

4. FINITE ELEMENT MODEL FOR END EFFECTOR

The end effector consists of a fire hose and the assembly components connecting it to an actuated arm. The fire hose is made up of EPDM rubber and nylon while the other components of the assembly are made up of aluminum. The fire hose has an EPDM internal bladder which expands with air pressure and a nylon exterior reinforced weave which protects the fire hose from bursting due to over pressurization. Key material properties are displayed in Table 1. For the fire hose, its material properties were estimated as a mixture of 90% Nylon and 10% EPDM. The end effector was simulated as an assembled system to see how the stresses react together. The material properties that were used are listed below.

Table 1. Material properties for FEA simulations [6, 7]

Material	Density (lb/in^3) / (kg/m^3)	Young's Modulus (KSI) / MPa	Poisson's Ratio
Aluminum	0.098 / 2712.631	1000 / 6894.760	0.334
Fire Hose	0.0392 / 1085.052	360.087 / 2482.712	0.4005

A general approach presented by Liu et al. [8-10] was followed to create the FEA models for the end effector and the fire hose, and all the simulations were completed in ABAQUS. As shown in Fig. 9, both models were meshed using C3D10 (a 10-node quadratic tetrahedron solid element). The two different element sizes 1.2 and 0.8 in (30.48 and 20.32 mm) were chosen for generating a variety of different meshes to evaluate the differences. This element size was determined after several element size sensitivity analysis to strike a balance between accuracy and efficiency of the FEA simulations [11-13]. Fig. 11 illustrates the loading and boundary conditions. Two different types of loading amplitudes were simulated to test if there were any differences in the results to protect for the loading to occur in different frequencies. The loading condition during the simulations is defined as follows: a pressure of 83 PSI (572 kPa) is applied on the hose contact area to generate a total force of 1000 lb (454 kg), which is exerted by the actuated arm moving the end effector down in the z-direction until the above pressures are reached. The hose contact area is 0.5 in (1.27 cm) wide and 24 in (61 cm) long. This is shown in a schematic in Fig. 10.

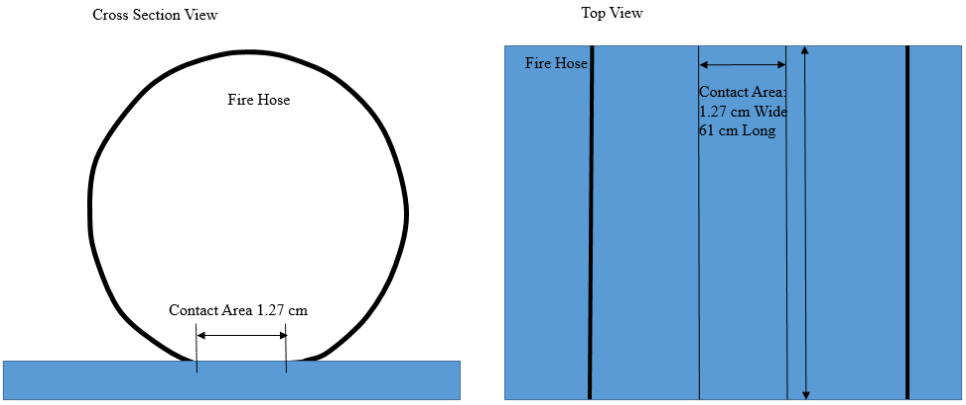

Figure 10. Schematic of contact area of fire hose

Simulation load condition: 1000 lb (454 kg), applied pressure over hose contact area:

$$\frac{1000lb}{0.5in \cdot 24in} = 83\ PSI$$

Which is 572 kPa over the hose contact area.

The simulation uses a tube for the fire hose, an exact 0.5 in (1.27 cm) contact area, and a clamped condition with the hose plate assembly; condition is no slip between the hose and hose plate, clamped condition between hose and hose plate assembly. The simulation is done using, first implicit model which is linear analysis then the results are compared with explicit dynamic analysis which is a nonlinear simulation. The assumption is that there is no slip between the fire hose and end effector. The tie condition was applied between the fire hose and end effector.

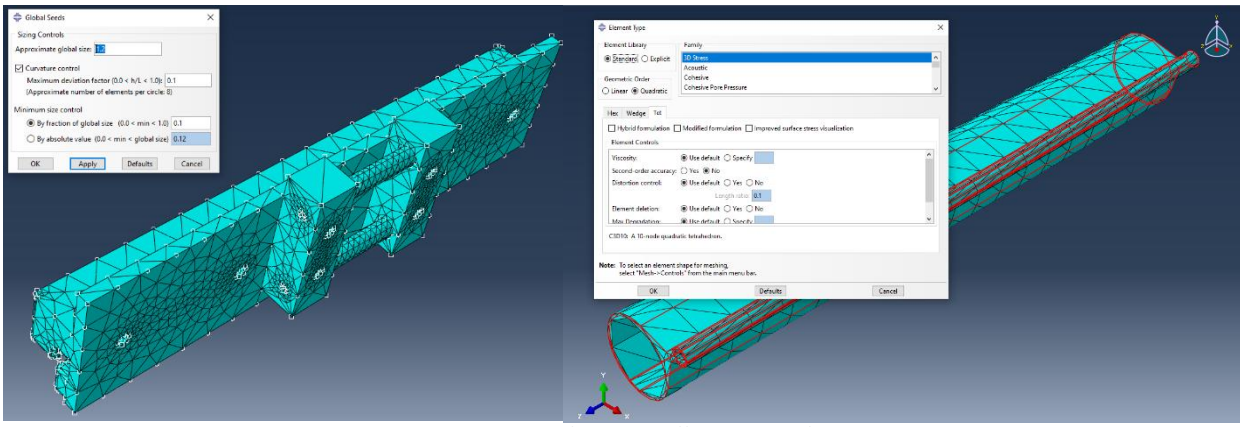

Figure 11. FEA models for the end effector and the fire hose

Load was applied from the bottom of the fire hose at 572 kPa and an internal fire hose pressure of 69 kPa was applied. Also, the right side of the end effector was fixed.

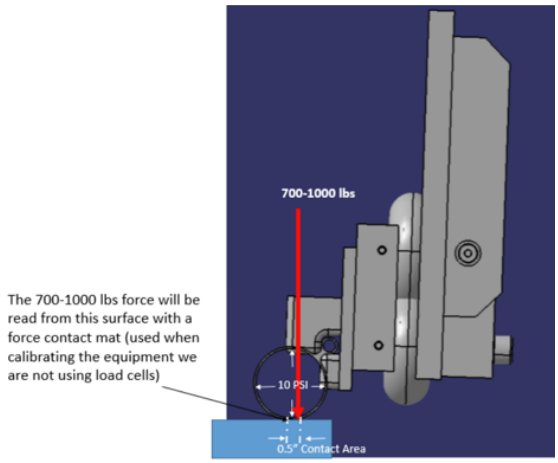

Figure 12. Loading conditions and boundary conditions

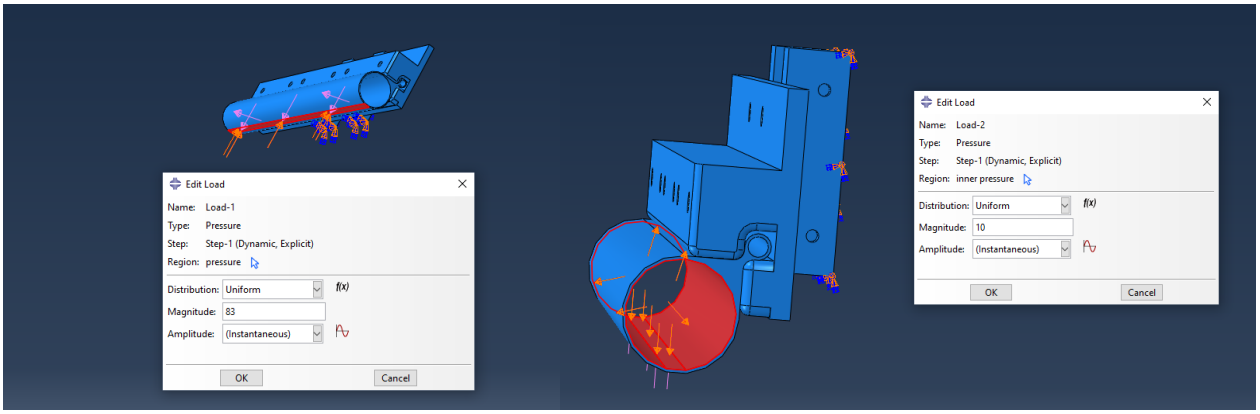

Figure 13. Applied loads and boundary conditions

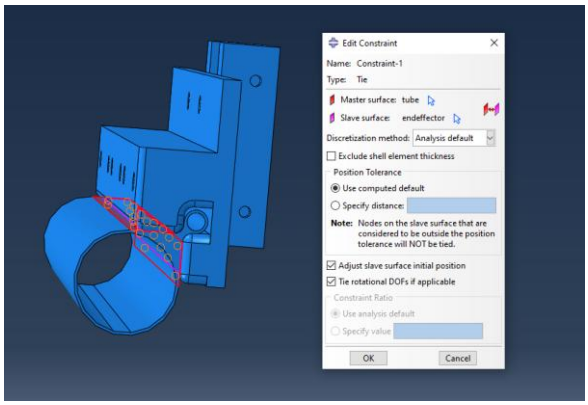

Figure 14. Tie condition between the fire hose and end effector

Key simulation parameters are listed in Table 2. The main purpose of this simulation is to see how the stress reacts together at different simulation approaches. Also, by decreasing mesh size, the optimal stress and deflection values were attempted to be solved.

Table 2. Set up and key parameters of FEA simulations

Cases	Analysis Type	Element Global Size (mm)	Time Period (sec)	Mass Scaling Factor	Load Amplitude
1	Implicit	30.48	1	N/A	Ramp
2	Implicit	20.32	1	N/A	Ramp
3	Explicit	20.32	0.09	No(1)	Smooth Step
4	Explicit	20.32	0.09	10	Smooth Step
5	Explicit	20.32	0.09	100	Smooth Step

5. RESULTS AND DISCUSSION

After completing the simulations, important results were extracted for each case and listed in table 3. As shown in that table, the maximum von Mises stress ranges from 3.29 to 13.51 kSI (22.47 to 93.15 MPa) and the maximum deflection varies from 0.06699 to 0.2968 inches (1.7 to 7.5 mm). Figs. 13 to 27 display the von Mises plots and deflection profiles obtained from each case.

The maximum von Mises stress occurs in Case 2; which has a global size of 20.32 mm. The higher observed stress is because of the smaller mesh size and the increased run time, which allowed the load to be applied evenly over one second. This allowed for a more accurate reading of stress. The lowest von Mises stress happens at Case 5; which had a global mesh size of 20.32 mm. The lower observed stress is primarily due to the increased mass scaling which scale the mass on a per step basis in a multistep analysis. An increase of the mass scaling increases the element-by-element stable time increment for an element set. This means that the elements were exposed to the load for a shorter amount of time. The smallest deflection of 1.701 mm happens at Case 1; which had a mesh size of 1.2 in (30.48 mm). However, when mesh size was decreased to 0.8 in (20.32 mm), the maximum deflection increased to 7.539 mm. Per mesh conversion approach, 7.539 mm value is considered a more accurate deflection value and

this implicit result is compared with the other explicit values for Cases 3, 4, and 5. Among them Cases 3 and 4 match well with implicit results. It can be assumed a mesh size of 1.2 in (30.48 mm) is too large and not able to observe all the deflection that is occurring since Cases 1 and 2 were identical in parameters except the size of the mesh and these resulted in the smallest and largest deflections.

Table 3. FEA simulation results

Cases	Max. Stress (Von-Mises) (MPa)	Max. Deflection (mm)
1	32.74	1.701
2	93.15	7.539
3	64.18	6.678
4	69.43	7.439
5	22.65	2.015

The below plot shows the max von Mises stress is 64.18 MPa at the shown location. This maximum stress happens inside the fire hose tube which is closed off to the end effector. This is expected since the pressure is being applied on the inner surfaces. The fire hose tensile strength is 137 MPa [14, 15], therefore it is within the range. Also, the highest stress is located at a stress concentration area, so it is safe to assume the fire hose is within an acceptable range of its maximum tensile strength. Case 4 max stress is a little higher than other explicit simulations, however the deflection is very close to case 2 and 3. Case 1 deflection is lowest.

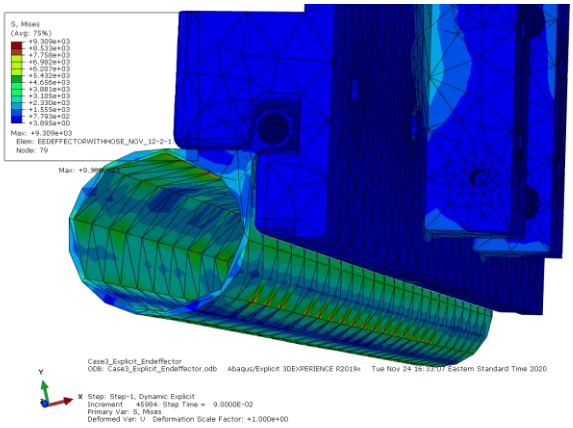

Figure 15: Max Stress at Case 3

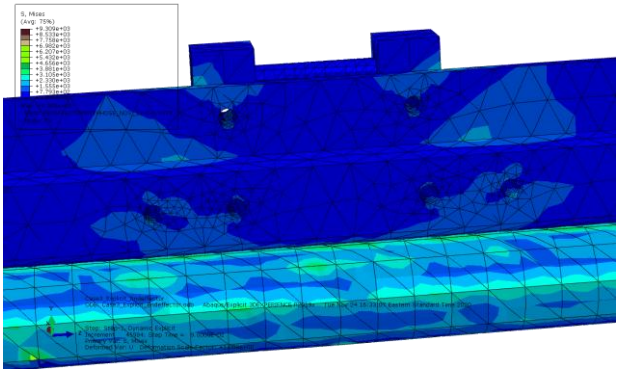

Figure 16: Von Mises Stress at Case 4

By looking at the different figures the majority of the end effector stress area is under 20 MPa, which is well under the fire hose and aluminum ultimate tensile strengths of 137 MPa and 310 MPa respectively. The below plot shows a max deflection of 6.678 mm in the shown location. The largest deflection happens at the contact area, which was anticipated because the contact area surface of the fire hose that is being pressed with 454 kg would indeed have the largest defection. This is not expected to be an issue while operating as it appears to be a reasonable amount of deflection and all the stresses are within the limits of the materials.

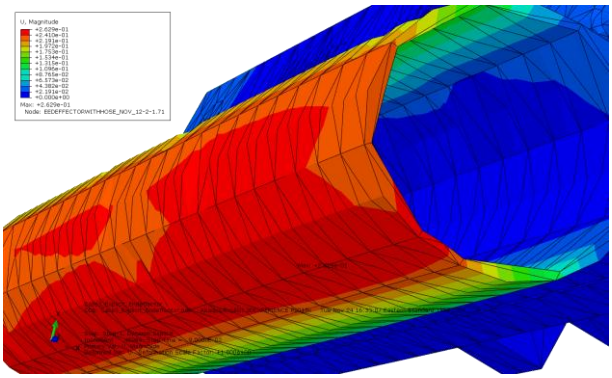

Figure 17: Max Deflection at Case 3.

Figure 17 shows case 3 which is representative of the explicit simulations. For Cases 3 and 4, the kinetic energies are relatively small compared to internal energies. Therefore Cases 3 and 4 simulations are considered close to quasi-static condition simulation, whereas Case 5 shows kinetic energy is higher by a significant amount, so it is not considered quasi-static simulation.

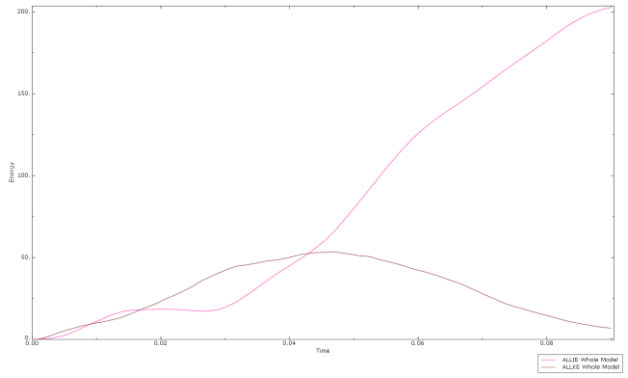

Figure 18: Case 4 Comparison of Internal energy and Kinetic energy

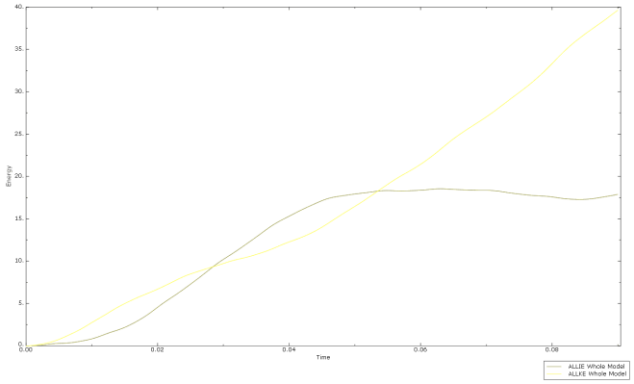

Figure 19: Case 5 Comparison of Internal energy and Kinetic energy

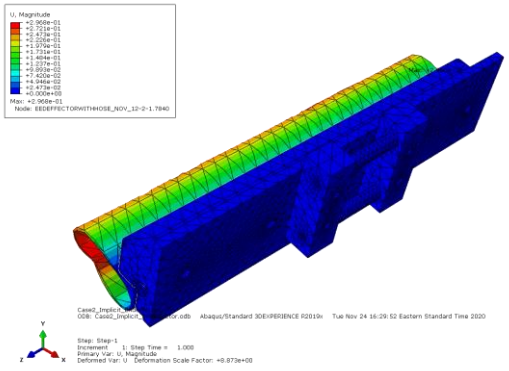

Figure 23: Case 2 Deflection Plot

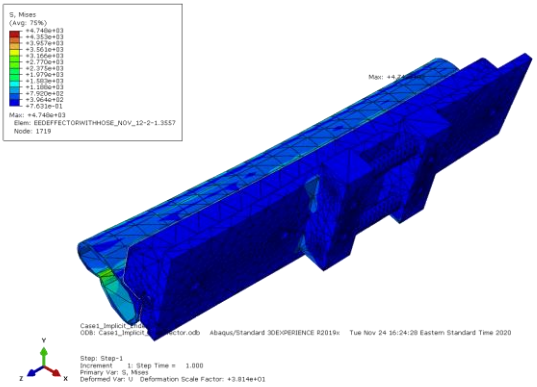

Figure 20: Case 1 Von-Mises Plot

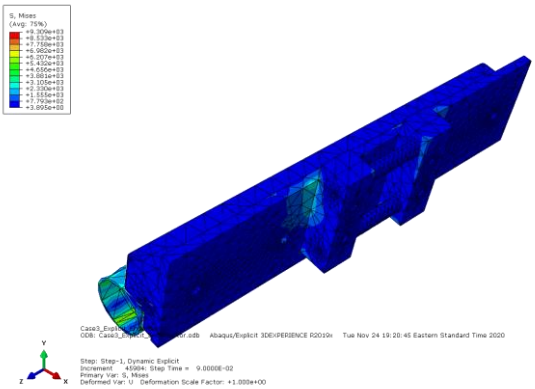

Figure 24: Case 3 Von-Mises Plot

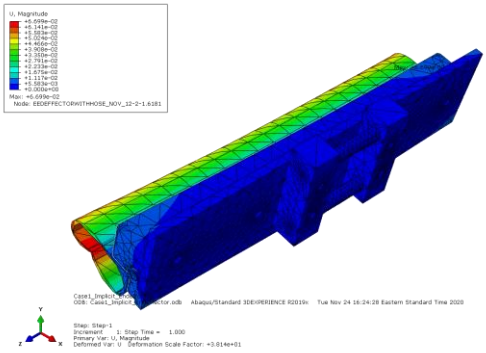

Figure 21: Case 1 Deflection Plot

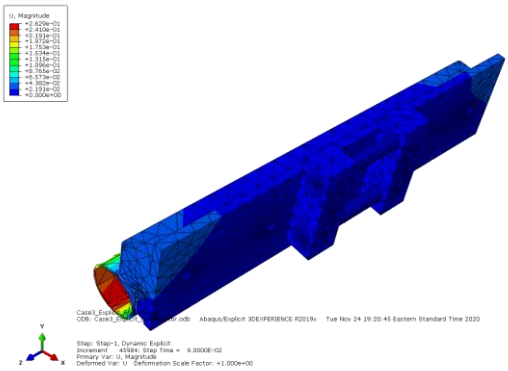

Figure 25: Case 3 Deflection

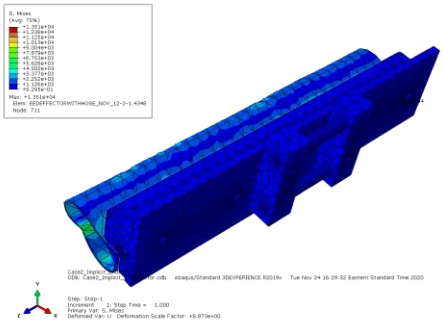

Figure 22: Case 2 Von-Mises Plot

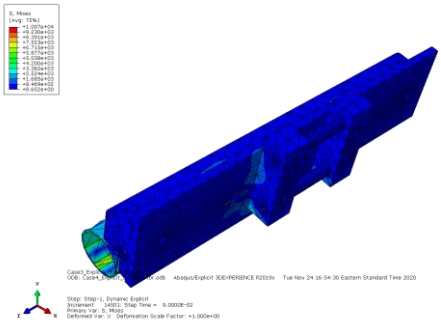

Figure 26: Case 4 Von-Mises Plot

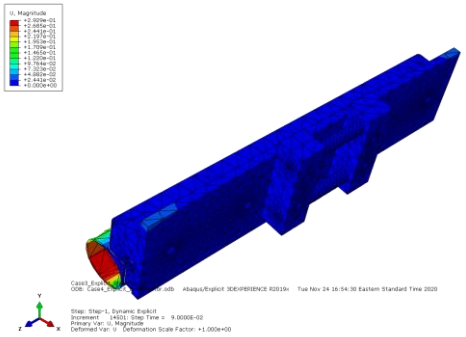

Figure 27: Case 4 Deflection Plot

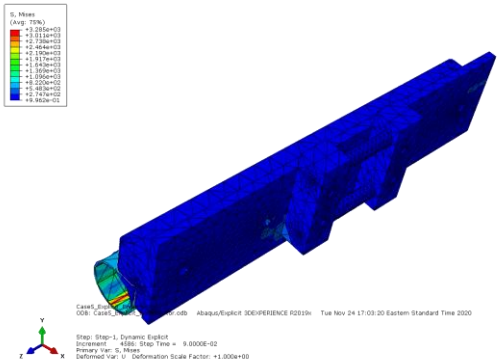

Figure 28: Case 5 Von-Mises Plot

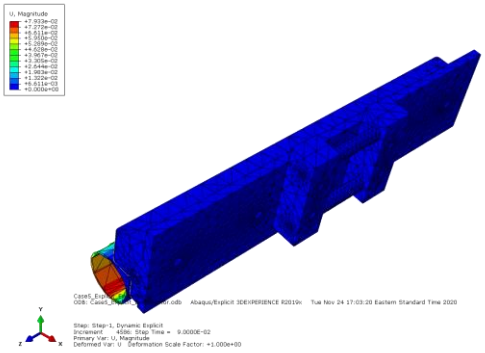

Figure 29: Case 5 Deflection Plot

6. CONCLUSIONS

A computational approach using finite element analysis (FEA) was used to examine the end effector materials and the assembly to confirm that they are robust enough to withstand the internal and external stresses and forces without failure or permanent deformation of the end effector materials, forces which are created from the pressurized fire hose and reactive force on the fire hose from the pressure being applied to an independent tool. From all the simulations it looks like the fire hose will undergo a sizable amount of deformation and stress. The aluminum is much lower on deformation scale and with stress around 20.684 MPa, it is not anticipated to be any issue in operation. Although the deformation and stress that the fire hose undergoes is not negligible, it should be low enough to proceed to test in real conditions. Especially considering the fact that this end effector will be tied to 5 additional end effectors which will help distribute the stress a bit. The desired effect of using a fire hose to be rigid yet forgiving seems to be confirmed with this simulation. The fire hose will be rigid and stiff when pressing and compacting the composite laminate but also forgiving so it may be possible to contour over curvatures and joggles. Whether or not this design will produce high quality composite materials is to be determined but this simulation has proven that it may be feasible.

7. REFERENCES

[1] Grant, C., "Automated processes for composite aircraft structure", *Industrial Robot*, Vol. 33 No. 2, 2006, 117-121.

[2] Willden, K.S., Van West, B.P., Harris, C.G., "Forming method for composites", US Patent No. 8,142,181, 2012.

[3] Reeves, J.A., Carlson, L.C., Pham, K.M., et. al., "Methods for forming a composite blade stiffener and facilitating application of barely visible impact damage treatments", US Patent No 10,377,091, 2019

[4] Talreja, Ramesh, "Manufacturing defects in composites and their effects on performance", *Polymer Composites in the Aerospace Industry*, 2015, 99-113

[5] Jareteg, Cornelia & Wärmefjord, Kristina & Cromvik, Christoffer & Söderberg, Rikard & Lindkvist, Lars & Carlson, Johan & Larsson, Stig & Edelvik, Fredrik. (2016). "Geometry Assurance Integrating Process Variation With Simulation of Spring-In for Composite Parts and Assemblies". *Journal of Computing and Information Science in Engineering*. 16. 10.1115/1.4033726.

[6] "Aluminum Mechanical Properties", *ASM Aerospace Specifications Metals Inc.*, http://asm.matweb.com/search/SpecificMaterial.asp?bassnum=MA6061T6. Accessed from 24 Aug 2021

[7] "Marco Rubber Compound # E1121 90 Durometer, Black, EPDM for Geothermal Applications Technical Datasheet" *Marco Rubber*, https://www.marcorubber.com/downloads/Marco-Material-Datasheet-E1121.pdf. Accessed from 24 Aug 2021

[8] Y.-C. Liu and Q.-K. Wang, "Computational study of strengthening effects of stiffeners on regular and arbitrarily stiffened plates", *Thin-Walled Structures*, 59, 2012, 78-86.

[9] Y.-C. Liu and M.L. Day, "Experimental analysis and computer simulation of automotive bumper system under impact conditions", *International Journal of Computational Methods in Engineering Science and Mechanics*, 9(1), 2008, 51-59.

[10] Y.-C. Liu, "Design enhancement of thin-walled steel beams with improved stiffness and reduced weight", *International Journal of Design Engineering*, 1(2), 2008, 149-165.

[11] Y.-C. Liu and G.A. Glass, "Effects of mesh density on finite element analysis", SAE Technical Paper 2013-01-1375, 2013.

[12] Y.-C. Liu, "ANSYS and LS-DYNA used for structural analysis", *International Journal of Computational Aided Engineering and Technology*, 1(1), 2008, 31-44.

[13] "Voloknohim Nylon Fiber 0.68 Tex", *MatWeb Material Property Data*, http://www.matweb.com/search/DataSheet.aspx?MatGUID=675b77f996b142f59e4cb60d69d64872&ckck=1. Accessed from 24 Aug 2021

[14] "High Tensile Strength Flexible Lightweight PU Fire Hose", *Quanzhou Winner Fire Fighting Equipment Co. Ltd.*, http://www.winnerfirehose.com/high-tensile-strength-flexible-lightweight-pu-fire-hose_p151.html. Accessed from 24 Aug 2021